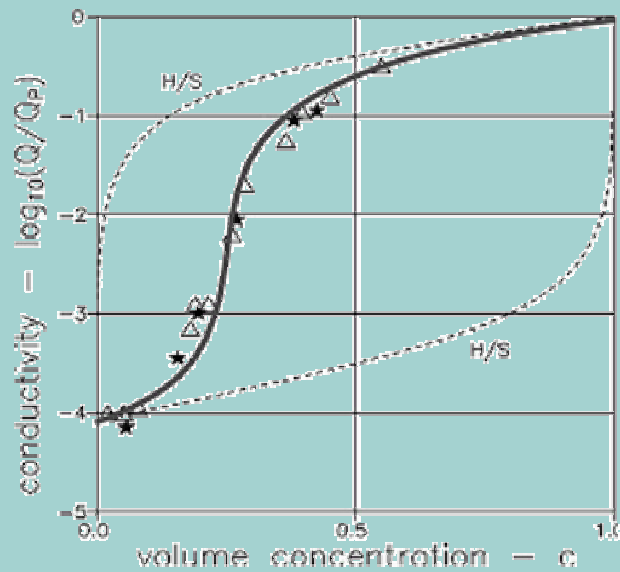


Lauge Fuglsang Nielsen

A composite theory and its potentials with respect to materials design



Rapport
BYG-DTU R-061

May 2003
ISSN 1601-2917
ISBN 87-7877-123-4

A composite theory and its potentials with respect to materials design

Lauge Fuglsang Nielsen

Abstract: An operational summary of a composite theory previously developed by the author is presented in this paper. Expressions are presented by which mechanical properties such as stiffness, eigenstrain/stress (e.g. shrinkage and thermal expansion), and physical properties (such as various conductivities with respect to heat, electricity, and chlorides) can be predicted for composite materials with variable geometries. Examples are presented, demonstrating an excellent agreement between material properties determined experimentally and such properties predicted by the theory considered.

In a special section of the paper the theory is examined with respect to its potentials with respect to materials design. Examples are presented, demonstrating how the method can be inverted to determine composite geometry from prescribed composite properties, such as Young's moduli and conductivities. Finally, research projects are suggested by which new production techniques might be found which are more rational than the ones known to day – and which could in a flexible way produce geometries determined by the inverse composite analysis indicated above.

A software, 'CompDesign' is prepared with application programs covering both the prediction aspects and the design aspects of the method presented. On special request the software is available contacting the author, lfn@byg.dtu.dk

Introduction

The composites considered in this paper are isotropic mixtures of two components: phase P and phase S. The amount of phase P in phase S is quantified by the so-called volume concentration defined by $c = V_P/(V_P+V_S)$ where volume is denoted by V. It is assumed that both phases exhibit linearity between response and gradient of potentials, which they are subjected to. For example: Mechanical stress versus deformation (Hooke's law), heat flow versus temperature, flow of electricity versus electric potential, and diffusion of a substance versus concentration of substance.

For simplicity – but also to reflect most composite problems encountered in practice – stiffness and stress results presented assume an elastic phase behavior with Poisson's ratios $\nu_P = \nu_S = 0.2$ (in practice $\nu_P \approx \nu_S \approx 0.2$). This means that, whenever stiffness and stress expressions are presented, they can be considered as generalized quantities, applying for any loading mode: shear, volumetric, as well as un-axial. This feature is explained in more details in a subsequent section (Composite analysis).

The composite properties specifically considered in this paper are stiffness, eigenstrain (such as shrinkage and thermal expansion), and various conductivities (with respect to chloride or heat flow e.g.) as related to volume concentration, composite geometry, and phase properties: Young's moduli E_P and E_S with stiffness ratio $n = E_P/E_S$, eigenstrains λ_P and λ_S , and conductivities Q_P and Q_S with conductivity ratio $n_Q = Q_P/Q_S$. Further notations used in the text are explained in the list of notations at the end of the paper.

The composite properties presented in this paper are determined by a general method developed by the author in (1,2,3). The strength of this method, including the present simplified

method, relative to other prediction methods with fixed, not variable types of composite geometries (such as plates or fibers in a matrix), is that global (standard) solutions are presented which apply for any isotropic composite geometry. The influence of geometries on material properties are 'hidden' in so-called 'geo-functions' (θ , see Equation 5) where specific geometries are quantified by so-called 'shape functions' (μ , see Figure 1 and Equation 4). Thus, properties can be predicted where geometry can be respected as it really develops in natural or man-made composite materials.

Not to exaggerate our present knowledge of composite geometries it has, deliberately, been chosen to keep the shape functions described by simple mathematical expressions defined by only three geometrical parameters (two shape factors and one critical concentration, see Equation 4 and Figure 1). It is emphasized, however, that the complexity of shape functions does not influence the global property predictions previously referred to. As more knowledge on the description of composite geometry turns up as the result of new research we just introduce the more 'accurate' shape functions.

It is emphasized that the paper is not a "textbook" in composite materials. It should rather be considered as an operational introduction to the basics of the composite analysis developed by the author – and to results, which can be obtained by such analysis. The text is rather brief, and no attempts have been made to explain expressions theoretically. Readers, interested in theoretical aspects are referred to the literature references presented along with the text.

Geometry

As demonstrated in Figure 1 composite geometry can be described by so-called shape functions which are determined by so-called shape factors (μ_P^0, μ_S^0) and critical concentrations, c_P and $c_S \leq c_P$: Shape factors tell about the shapes of phase components at dilute concentrations. Critical concentrations are concentrations where the composite geometry changes from one type to another type.

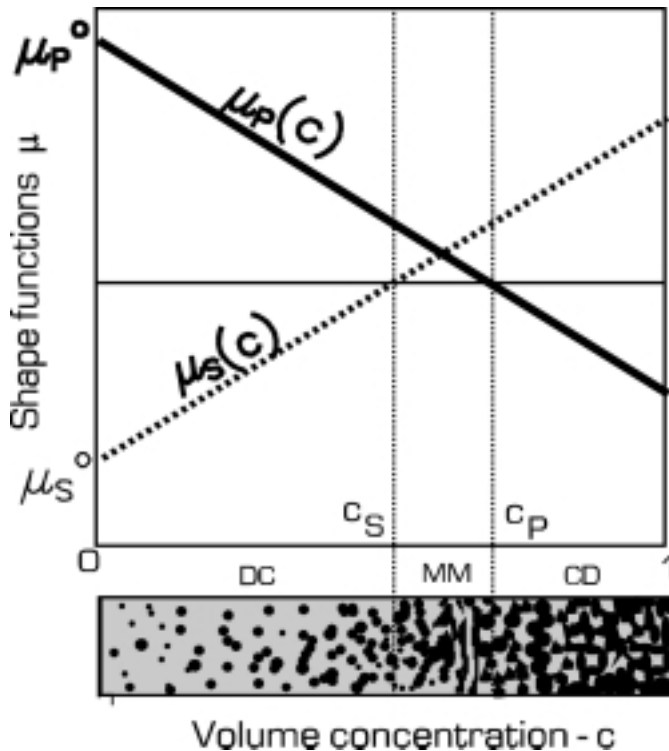


Figure 1. Geometrical significance of shape functions. $(\mu_P, \mu_S) = (+, -)$ means discrete P in continuous S . $(\mu_P, \mu_S) = (+, +)$ means mixed P in mixed S . $(\mu_P, \mu_S) = (-, +)$ means continuous P with discrete S . Black and gray signatures denote phase P and phase S respectively. (μ_P^0, μ_S^0) are so-called shape factors. (c_P, c_S) are so-called critical concentrations.

At fixed concentrations we operate with the following types of composite geometries: DC means a discrete phase P¹⁾ in a continuous phase S. MM means a mixed phase P geometry in a mixed phase S geometry, while CD means a continuous phase P mixed with a discrete phase S. We notice that MM-geometries (if porous) are partly impregnable. In modern terminology this means that phase P percolation exists in composites with $c > c_S$. Percolation is complete for $c \geq c_P$. Porous materials have lost any coherence in this concentration area with no stiffness and strength left.

Composite geometries may change as the result of volume transformations associated with increasing phase P concentration. We will think of changes as they are stylized in Figure 1: At increasing concentration, from $c = 0$, discrete P elements agglomerate and change their shapes approaching a state at $c = c_S$ where they start forming continuous geometries. Phase P grows fully continuous between $c = c_S$ and $c = c_P$ such that the composite geometry from the latter concentration has become a mixture of discrete, de-agglomerating, phase S particles in a continuous phase P.

In a complementary way the geometry history of phase S follows the history of phase P and vice versa. The geometries just explained can be shifted along the concentration axis. A composite may develop from having a DC geometry at $c = 0$ to having a MM geometry at $c = 1$. Such composite geometries, with $c_P > 1$ and $0 < c_S < 1$, are named DC-MM geometries. Other composites may keep their DC type of geometry all the way up to $c = 1$ in which case the composite geometry is denoted as a DC-DC geometry, with both critical concentrations > 1 . The geometry outlined in Figure 1 changes from DC to CD geometry which makes it a DC-CD geometry with both critical concentrations in $c = 0-1$.

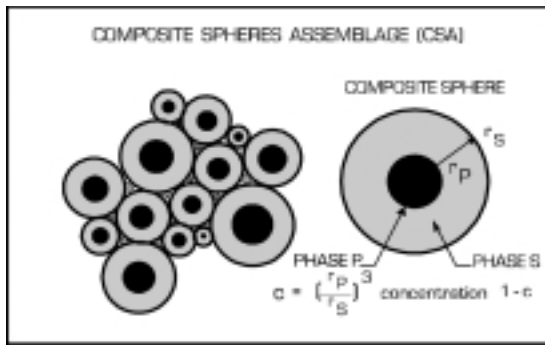


Figure 2. Composite spherical assemblage with phase P particles, CSA_P .

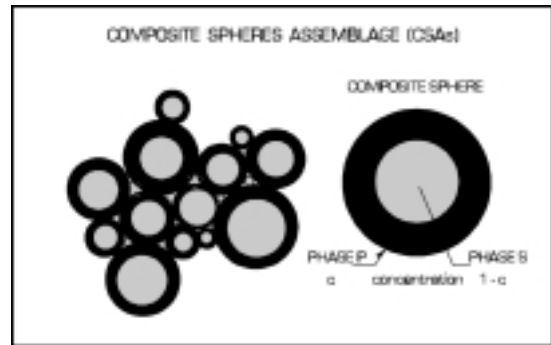


Figure 3. Composite Spheres Assemblage with phase S particles, CSA_S .

Remark: Ideal geometries at $c = 0$ and at $c = 1$ of a DC-CD composite are illustrated in Figures 2 and 3 respectively. We notice in this context that the composite theory developed in (1,2,3) is based on the concept that any isotropic composite geometry is a station on a geo-path moving from the CSA_P geometry shown in Figure 2 to the CSA_S geometry shown in Figure 3. CSA is an abbreviation for the composite model Composite Spheres Assemblage introduced by Hashin in (4). It is noticed that the four letter symbols for composite

¹ A phase with continuous geometry (C) is a phase in which the total composite can be traversed without crossing the other phase. This is not possible in a phase with discrete geometry (D). A mixed geometry (M) is a continuous geometry with some discrete elements.

geometries are subsequently also used in the meaning, for example: a 'DC-CD type of composite', a 'DC-CD type of geometry', or just a 'DC-CD composite'.

Composites considered

The various types of geometries considered are listed in Figure 4 which defines the following two composite classes considered in this paper: *Particulate composites* are defined by the former row. They have particles in a matrix geometry (DC) at small concentrations. *Lamella composites* are defined by the latter row. They have a mixed phase P geometry in a mixed phase S geometry (MM) at low concentrations. Obviously, the phenomenon of percolation previously considered develops between the two critical concentrations. In Figure 4 gray shadings indicate the phase P percolation. We assume that percolation varies linearly from being 0 at $c < c_S$ to being 100% at $c > c_P$.

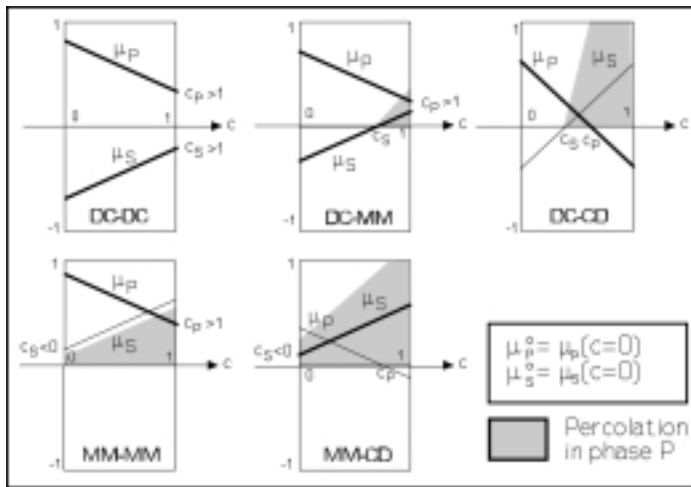


Figure 4. Composite types versus critical concentrations. Former and latter two letters denote composite geometry at $c = 0$ and at $c = 1$ respectively.

TYPE		EXAMPLES
DC	DC	Particulate composite (concrete, mortar). Extremely high quality of grading (approaching CSA_P composites). <i>Pore system:</i> Not impregnable. Finite stiffness at any porosity
	MM	Particulate composite (concrete, mortar) with particle interference at $c = c_S$. Increasing quality of grading is quantified by larger concentration c_S at first severe interference. <i>Pore system:</i> Only impregnable for porosities $c > c_S$. Finite stiffness at any porosity.
	CD	Mixed powders (ceramics). <i>Pore system:</i> Only impregnable for porosities $c > c_S$. No stiffness for porosities $c > c_P$.
MM	MM	Mixed lamella/foils ("3D-plywood"). <i>Pore system:</i> Fully open at any porosity. Finite stiffness at any porosity.
	CD	Mixed lamella/foils ("3D-plywood"). <i>Pore system:</i> Fully open at any porosity. No stiffness for porosities $c > c_P$.

Table 1. Examples of composites outlined in Figure 4.

Quantification of composite geometry

Shape factors

Shape factors for *particulate composites* with plain fiber/disc particles can be accurately determined by Equation 1, reproduced from (3)² where particle shapes are quantified by the aspect ratio, $A = \text{length/diameter}$ of particle. Spherical particles have $A = 1$. Long particles have $A > 1$. Flat particles have $A < 1$.

$$\mu_p^o = \begin{cases} \frac{3A}{A^2 + A + 1} & ; A \leq 1 \\ 3 \frac{A^2 - A + 1}{4A^2 - 5A + 4} & ; A > 1 \end{cases} ; \mu_s^o = - \begin{cases} \mu_p^o & ; A \leq 1 \\ 4 \mu_p^o - 3 & ; A > 1 \end{cases} \quad \text{one shape} \quad (1)$$

For particulate composites with phase P being a mixture of particles with various aspect ratio distributions the shape factors can be accurately calculated by a method developed in (3). For the case of mixtures with only two aspect ratios this method is included as part of the sub program 'Comp' in 'CompDesign' previously referred to. An example: A mixture made with 20% $A = 0.3$ and 80% $A = 2$ is characterized by the shape factors $(\mu_p^o, \mu_s^o) = (0.83, -0.68)$.

An approximate determination of shape factors for a two-shape (A_1, A_2) particulate composite can be obtained by the following expression, where α_1 is volume fraction of particles with aspect ratio A_1 while $(\mu_{p1}^o, \mu_{s1}^o, \mu_{p2}^o, \mu_{s2}^o)$ are shape factors individually determined by Equation 1 for the two aspect ratios.

$$\mu_p^o \approx \left(\frac{\alpha_1}{\mu_{p1}^o} + \frac{1 - \alpha_1}{\mu_{p2}^o} \right)^{-1} \quad \mu_s^o \approx \left(\frac{\alpha_1}{\mu_{s1}^o} + \frac{1 - \alpha_1}{\mu_{s2}^o} \right)^{-1} \quad \text{two shapes} \quad (2)$$

Shape factors for *laminar composites* are estimated as explained in a subsequent section.

Critical concentrations

It is emphasized that the critical concentrations depend very much on the processing technique used to produce composites. We notice that particle size distribution is part of processing. For particulate composites, for example, the critical concentration c_s can be thought of as the concentration at first severe interference of phase P (starting the creation of a continuous skeleton). Improved quality of size distribution (smoothness and density) is considered by increasing c_s . At this concentration porous materials become very stiff when impregnated with a very stiff material. At the other critical concentration, $c = c_p$, the composite becomes a mixture of phase S elements completely wrapped in a matrix of phase P. As previously mentioned porous materials lose their stiffness and strength at c_p because phase P has become a continuous, enveloping, void system.

Remark: The definition of interference ('severe') introduced above is kept throughout the paper. It is implicitly assumed that particles at $c > c_s$ are kept together by a very thin, sufficiently strong matrix "glue".

² Modified version of a similar expression presented in (2).

As previously indicated, critical concentrations can be fictitious (outside $c = 0 - 1$). In such cases they do not, of course, have the immediate physical meanings just explained. Theoretically, however, if we think of the c -axis as a plain geometry axis we may keep the explanation given in order to describe in an easy way, how the rate of changing the composite geometry is influenced by the processing technique used. In such fictitious cases critical concentrations will have to be estimated from experience, or detected from calibration experiments.

Geo-path

A geo-path defines the type of composite geometry as it develops when the volume concentration of phase P increases from $c = 0$ to $c = 1$. Obviously this 'history' is a matter of production technology, which cannot be studied by theoretical means only. Reasonable estimates, however, can be made (3) from knowing about shape factors (shape function values at $c = 0$) and from knowing about critical concentrations (where one shape function value is 0). The geo-path shown in Figure 5 is reproduced from (3,5) assuming a production technology that can produce geometries (shapes) for which shape function values are related by the

$$\text{Geo-path : } \mu_S = a - \mu_P; \text{ with a path factor of } a = \mu_P^o + \mu_S^o \quad (3)$$

compiling the following shape functions with one known critical concentration (c_P or c_S) estimated from experience,

$$\mu_P = \mu_P^o \left(1 - \frac{c}{c_P} \right); \mu_S = \text{MIN} \left(\frac{\mu_S^o (1 - c/c_S)}{1} \right) \text{ with } \frac{c_P}{c_S} = - \frac{\mu_P^o}{\mu_S^o} \quad (4)$$

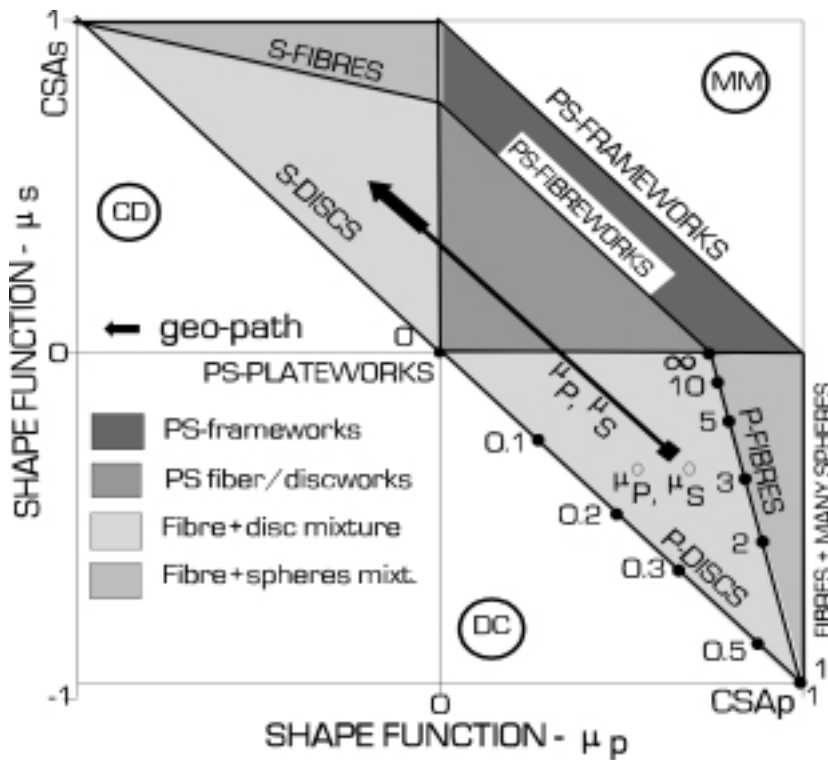


Figure 5. Geo-path and qualitative description of geometries: Numbers indicate fiber aspect ratio A of phase P particles. In section CD aspect ratios of phase S particles are symmetrical with respect to $\mu_P = \mu_S$. Frame- and fiber works are agglomerating MM-structures of long crumbled fibers and shorter crumbled fibers respectively. Disc works are agglomerating MM-structures of crumbled discs (sheets). Plate works are crumbled sheets (foils).

Remark: The geo-path suggested in Equation 4 has been successfully applied in (2,3) on a number of composites made with traditional technologies: Particles mixed into a continuous matrix, compaction of powders, production of porous materials, impregnation of porous materials, particulate composites with self-inflicted pores (light clinker concrete), three dimensional ‘Plywood’ composites.

Composite analysis

The preparation of a composite analysis is as follows:

- For particulate composites, calculate shape factors (μ_P^0, μ_S^0) from Equations 1 and 2. For lamella composites, use Figure 5 to estimate ($\mu_P^0 > 0$ and $\mu_S^0 > 0$) with μ_P^0 increasing from 0 for plate works to 1 for open frame works.
- Then decide the critical concentration c_S (or c_P) from knowing about mixing technology and observations made on geometrical formation.
- Now composite geometry can be quantified as expressed by the shape functions presented in Equation 4.
- The last step of preparing a composite analysis by the global solutions (valid for any geometry) presented in Equations 6 to 10 is to calculate the so-called geo-functions expressed by Equation 5 for stiffness analysis and conductivity analysis respectively.

Geo - function for stiffness analysis :

$$\theta = \frac{1}{2} \left[\mu_P + n\mu_S + \sqrt{(\mu_P + n\mu_S)^2 + 4n(1 - \mu_P - \mu_S)} \right] ; n = \frac{E_P}{E_S} \quad (5)$$

Geo - function for conductivity analysis :

$$\theta_Q = \mu_P + n_Q\mu_S + \sqrt{(\mu_P + n_Q\mu_S)^2 + 4n_Q(1 - \mu_P - \mu_S)} ; n_Q = \frac{Q_P}{Q_S}$$

Composite properties

With composite geometry described by the geo-functions presented in Equation 5 a property analysis can now be made using the following global solutions 6 - 10 with symbols explained in the list of notations presented at the end of the paper.

Remark: We re-call from the introduction that the stiffness- and stress expressions presented have a generalized meaning. They can be used for any loading mode, shear, volumetric, as well as uni-axial. For example, E/E_S can also be used to predict the composite shear modulus, G/G_S , and the composite bulk modulus, K/K_S , normalized with respect to the phase S properties. In a similar way the phase stresses, σ_P/σ and σ_S/σ , also apply independently of loading mode as long as both phase stress modes (σ_P, σ_S) and composite (external) stress modes (σ) are the same.

Stiffness and eigenstrain/stress

Stiffness

$$e = \frac{E}{E_S} = \frac{n + \theta [1 + c(n - 1)]}{n + \theta - c(n - 1)} \quad (6)$$

Stress due to external mechanical load

$$\frac{\sigma_P}{\sigma} = \frac{n(1 + \theta)}{n + \theta[1 + c(n - 1)]} ; \quad \frac{\sigma_S}{\sigma} = \frac{n + \theta}{n + \theta[1 + c(n - 1)]} \quad (7)$$

Eigenstrain - linear

$$\lambda = \lambda_S + \Delta \lambda \frac{1/e - 1}{1/n - 1} ; \quad (\Delta \lambda = \lambda_P - \lambda_S) \quad (8)$$

Eigenstress – hydrostatic

$$\rho_P = -\frac{5}{3} E_S \Delta \lambda \frac{c(1/n - 1) - (1/e - 1)}{c(1/n - 1)^2} ; \quad \rho_S = -\frac{c}{1 - c} \rho_P \quad (9)$$

Conductivity

$$q = \frac{Q}{Q_S} = \frac{n_Q + \theta_Q [1 + c(n_Q - 1)]}{n_Q + \theta_Q - c(n_Q - 1)} \quad (10)$$

Bounds on stiffness and conductivity

It comes from (1,2,3) that the above predictions are bounded as follows between the exact solutions for the CSA composite illustrated in Figures 2 and 3.

$$\frac{n + 1 + c(n - 1)}{n + 1 - c(n - 1)} \leq e = \frac{E}{E_S} < n \frac{2 + c(n - 1)}{2n - c(n - 1)} \quad (11)$$

valid for $n \geq 1$; reverse signs when $n < 1$

The stiffness bounds are obtained introducing $\theta \equiv 1$ and $\theta \equiv n$ respectively into Equation 6. The conductivity bounds are obtained introducing $\theta_Q \equiv 2$ and $\theta_Q \equiv 2n_Q$ respectively into Equation 10. The bounds such determined are the same as can be obtained from the studies made by Hashin and Shtrikman in (6) on composite stiffness and in (7) on composite conductivity. The bounds just considered are subsequently referred to by H/S.

$$\frac{n_Q + 2[1 + c(n_Q - 1)]}{n_Q + 2 - c(n_Q - 1)} \leq q = \frac{Q}{Q_S} \leq n_Q \frac{3 + 2c(n_Q - 1)}{3n_Q - c(n_Q - 1)} \quad (12)$$

valid for $n_Q \geq 1$; reverse signs when $n_Q < 1$

Examples

Three examples are presented in this section where composites are subjected to a property analysis as it has been presented in this paper. The text of the examples is very short. Only information absolutely necessary for solving the problems is presented. Other examples of property predictions are presented in (8,3).

Thermal expansion of salt infected bricks

The dotted data shown in Figure 6 are from an experimental study reported in (9) on damage of bricks caused by salt intrusion. The solid line data are the results of a composite analysis with the following component properties justified in (3). Additional results from the analysis are the internal stresses presented in Figure 7.

Composite: CC-CD with $(\mu_P^\circ, c_P) = (0.9, 0.53)$ and estimated $\mu_S^\circ = 0.05$
Phase S (Tile): $E_S = 38000$ MPa, $\lambda_S = 6 \cdot 10^{-6}/^\circ\text{C}$

Phase P (Salt): $E_p = 20000 \cdot \beta / (2 - \beta)$ MPa, (degree of pore impregnation: $\beta = 0.15 - 0.25$)
 $\lambda_p = 3.8 \cdot 10^{-5} / ^\circ\text{C}$

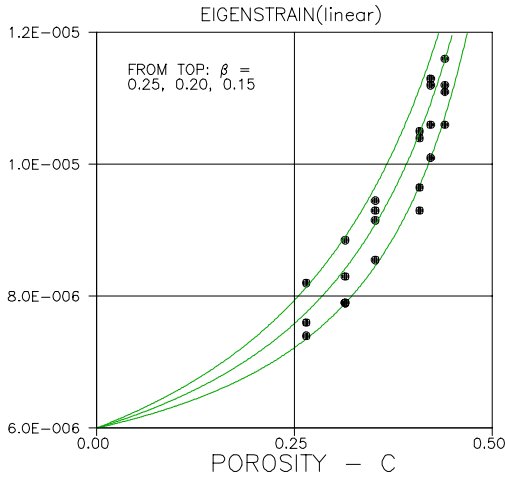


Figure 6. Thermal eigenstrain ($^\circ\text{C}$) of salt infected tile.

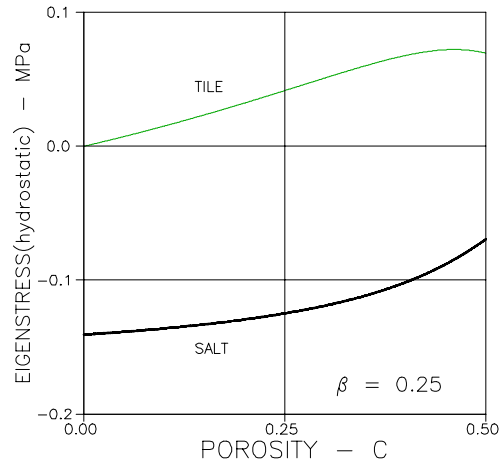


Figure 7. Predicted thermal eigenstresses ($^\circ\text{C}$) in salt infected brick.

Stiffness of – and diffusion coefficient (Chloride) in cement paste system

Phase properties: The components are phases (P,S) = (saturated capillary pores, cement gel). The Young's moduli and the Chloride diffusion coefficients are $(E_p, E_s) = (0, 32000)$

MPa and $(Q_p, Q_s)/Q_p = (1, 0.00008)$ respectively (with $Q_p = 2 \cdot 10^{-9} \text{ m}^2/\text{sec}$). These data are deduced from stiffness experiments reported in (10,11) and chloride diffusion experiments reported in (12,13).

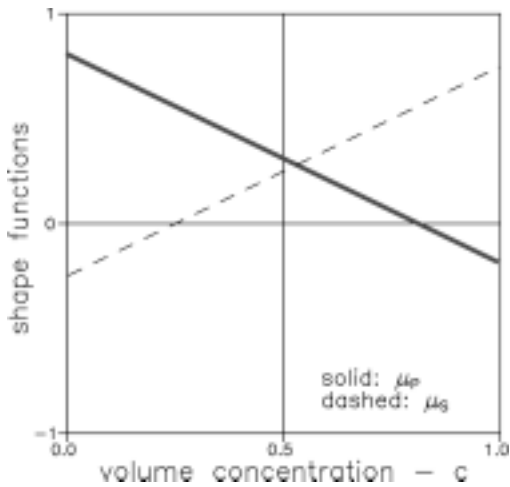


Figure 8. Cement paste considered: Geometry of cement paste considered.

Geometry: We estimate that pores, at an average, have an aspect ratio of $A = 4$ at low porosities. Shape factors of $(\mu_p^0, \mu_s^0) = (0.81, -0.25)$ are then calculated by Equation 1. A critical concentration of $c_p = 0.78$ is estimated from (14) where it was shown that cement paste exhibits no stiffness (and strength) at porosities greater than $c \approx 0.78$. (The solid phase (S) becomes surrounded by voids at that concentration). From Equation 4 we get $c_s = 0.24$.

Equation 4 now determines the shape functions presented in Figure 8. The composite analysis proceeds exactly as explained in the previous section of the paper. The results are shown in Figures 9 and 10 together with test data from (10,11,15,13).

Remarks: It is of some interest to compare the results just obtained with Figures 11 and 12 presenting predictions assuming two other composite geometries:

- 1) *DC-CD composite with compacted spheres:* (In the present theory quantified by $(A, c_s) = (1, 0.5) \Rightarrow \mu_p = 1 - 2c$ and $\mu_s = 2c - 1$). The stiffness prediction for this geometry can be presented in a closed analytical form, namely Equation 13, which according to (1) is identical to a solution, which can be obtained from the analysis of Budiansky (16).

$$e = \frac{1}{2} \left[(1 - n)(1 - 2c) + \sqrt{(1 - n)^2(1 - 2c)^2 + 4n} \right] \quad (13)$$

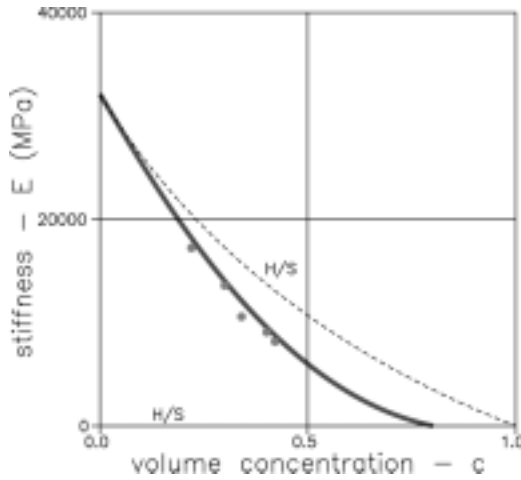


Figure 9. Cement paste system considered: Stiffness as related to capillary porosity, present analysis.

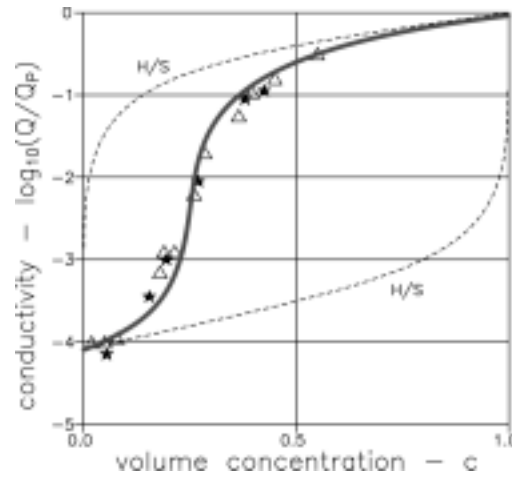


Figure 10. Cement paste system considered: Chloride diffusivity as related to capillary porosity, present analysis.

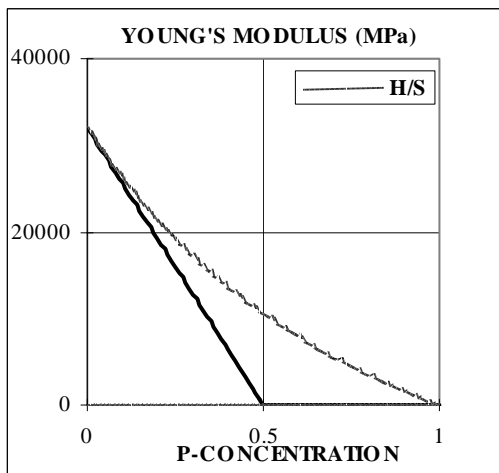


figure 11. Cement paste system considered with other geometries as explained in the text: solid line is Geometry 1. Dashed line is Geometry 2.

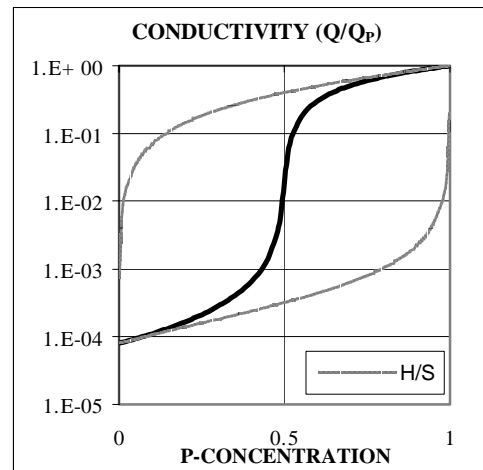


figure 12. Cement paste system considered with other geometries as explained in the text: solid line is Geometry 1. Lower dashed line is Geometry 2.

- 2) DC-DC composite with P-spheres in a continuous S-matrix, see Figure 2: (In the present theory quantified by $(A, c_s) = (1, \infty) \Rightarrow \mu_p \equiv 1$ and $\mu_s \equiv -1$). The stiffness prediction for this geometry can also be given a closed analytical form, namely Equation 11(left side), which according to (1) is identical to the CSA_p solution previously referred to by Hashin (4). We notice that geometry 2) equals one of the H/S bounds previously referred to.

We notice from Figures 9 – 12 that the influence of composite geometries 1) and 2) on composite properties are very different from the influence of the geometry applying for the composite system considered in this example.

Conclusion on property prediction

The statement, that composite properties depend very much on composite geometry has been convincingly confirmed and quantified in (1,2,3,8) demonstrating a very satisfying agreement between theoretically predicted data and experimentally obtained data reported in the composite literature.

It is emphasized that the basic prediction expressions presented are global, meaning that they apply for any isotropic composite geometry.

Aspects of materials design

The quality of the present theory to work with global descriptions (θ) of composite geometries qualifies it to be used in design of composite materials, meaning that geometries can be found which associate with prescribed composite properties. We just have to make an inverse analysis of the composite expressions previously presented. Keeping our source materials, Phase P and Phase S, such analysis can be made by the following expressions applying for any geo-path.

Geo-function versus properties (from Equations 6 and 10)

$$\theta = \frac{[n - c(n - 1)]e - n}{1 + c(n - 1) - e} \quad \text{Stiffness} \quad (14)$$

$$\theta_Q = \frac{[n_Q - c(n_Q - 1)]q - n_Q}{1 + c(n_Q - 1) - q} \quad \text{Conductivity}$$

Shape functions versus geo-functions (from Equation 5)

$$\theta = \frac{1}{2} \left[\mu_P + n \mu_S + \sqrt{(\mu_P + n \mu_S)^2 + 4n(1 - \mu_P - \mu_S)} \right] \text{ is a root in} \quad \text{Stiffness} \quad (15)$$

$$\theta^2 - \theta(\mu_P + n \mu_S) - n(1 - \mu_P - \mu_S) = 0 \text{ relating } \mu_P \text{ and } \mu_S \text{ by}$$

$$\mu_S = \frac{n(1 - \mu_P) - \theta(\theta - \mu_P)}{n(1 - \theta)} \text{ or } \mu_P = \frac{n(1 - \mu_S) - \theta(\theta - n \mu_S)}{n - \theta}$$

$$\theta_Q = \mu_P + n_Q \mu_S + \sqrt{(\mu_P + n_Q \mu_S)^2 + 4n_Q(1 - \mu_P - \mu_S)} \text{ is a root in} \quad \text{Conductivity} \quad (16)$$

$$\theta_Q^2 - 2\theta_Q(\mu_P + n_Q \mu_S) - 4n_Q(1 - \mu_P - \mu_S) = 0 \text{ relating } \mu_P \text{ and } \mu_S \text{ by}$$

$$\mu_S = \frac{4n_Q(1 - \mu_P) - \theta_Q(\theta_Q - 2\mu_P)}{2n_Q(2 - \theta_Q)} \text{ or } \mu_P = \frac{4n_Q(1 - \mu_S) - \theta_Q(\theta_Q - 2n_Q \mu_S)}{2(2n_Q - \theta_Q)}$$

Remark: We notice that a number of possibilities of shape function values are possible for predicting prescribed material properties: For each μ_P there is a μ_S .

Illustrative example

As previously indicated Equations 14 – 16 apply for any geo-path, $\mu_S = f(\mu_P)$. In order to simplify matters, however, we will demonstrate the design procedure applying the simple path $\mu_P + \mu_S = a$ defined by the so-called geo-path factor, $0 \leq a \leq 1$.

One prescribed property: With a prescribed Young's modulus of E^* , or conductivity Q^* , at volume concentration c^* the shape function values are determined as follows, meaning that one data set (μ_P^*, μ_S^*) on the geo-graph is presented.

$$\theta^* = \frac{[n - c^*(n-1)] e^* - n}{1 + c^*(n-1) - e^*} \Rightarrow \text{Stiffness} \quad (17)$$

$$\mu_S^* = \frac{n(1-a) + \theta^*(a - \theta^*)}{\theta^*(1-n)} : \mu_P^* = a - \mu_S^*$$

$$\theta^*_Q = \frac{[n_Q - c^*(n_Q-1)] q^* - n_Q}{1 + c^*(n_Q-1) - q^*} \Rightarrow \text{Conductivity} \quad (18)$$

$$\mu_S^* = \frac{4n_Q(1-a) + \theta^*_Q(2a - \theta^*_Q)}{2\theta^*_Q(1-n_Q)} : \mu_P^* = a - \mu_S^*$$

Two prescribed properties: With two prescribed Young's moduli, E_1 and E_2 , or conductivities Q_1 and Q_2 , at volume concentrations, c_1 and c_2 respectively the shape function values (μ_{P1}, μ_{S1}) and (μ_{P2}, μ_{S2}) are determined. Assuming that the same geo-path factor, a , applies for both analysis, the full shape functions (μ_P, μ_S) can be determined using that the shape functions vary linearly with volume concentrations. This means that the full geo-path, $\mu_S = f(\mu_P)$ can be presented. We will demonstrate this feature by two examples:

Example 1 (Stiffness)

Sources: $(E_P, E_S) = (0, 32000)$ MPa

Geo-path factor: $a = 0.5$.

Prescribed Young's moduli: $(E_1, E_2) = (12500, 5000)$ MPa at $(c_1, c_2) = (0.3, 0.5)$.

Results of analysis: Figures 13 and 14.

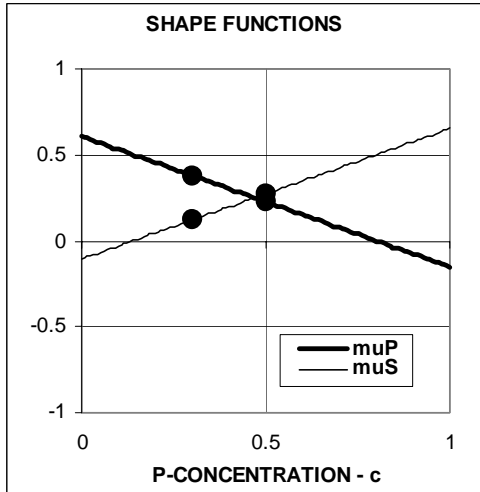


Figure 13. Shape functions in stiffness analysis

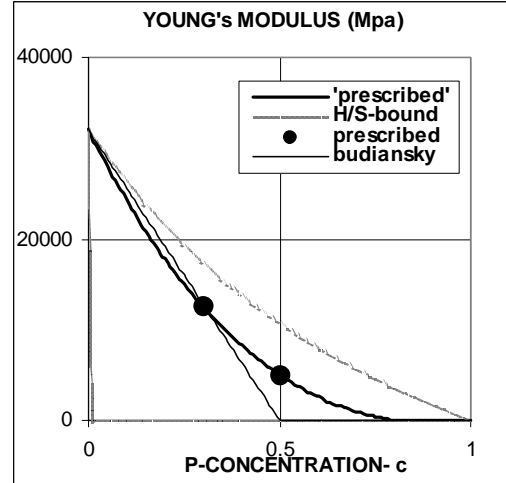


Figure 14. Stiffness analysis.

Evaluation of geometry:

The shape functions presented in Figure 13 are easily transformed to the geo-path graph shown in Figure 17. The prescribed stiffness data are properties of a composite

produced with geometries described placing Figure 17 on top of the master path graph in Figure 5.

Example 2 (Conductivity)

Sources: $(Q_P, Q_S)/Q_P = (1, 0.00008)$ with $Q_P = 2 \cdot 10^{-9} \text{ m}^2/\text{sec}$

Geo-path factor $a = 0.9$.

Prescribed conductivities: $(Q_1, Q_2)/Q_P = (0.001, 0.1122)$ at $(c_1, c_2) = (0.19, 0.43)$.

Results of analysis: Figures 15 and 16.

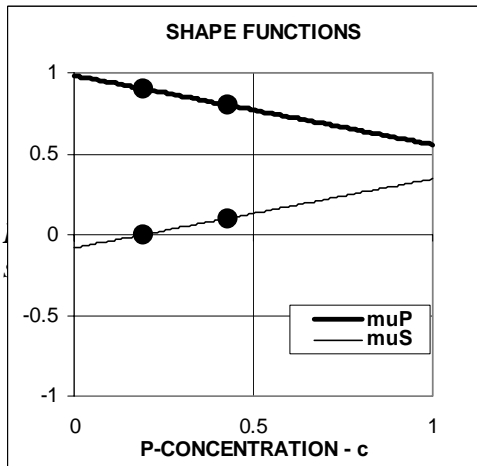


Figure 15. Shape functions in conductivity analysis

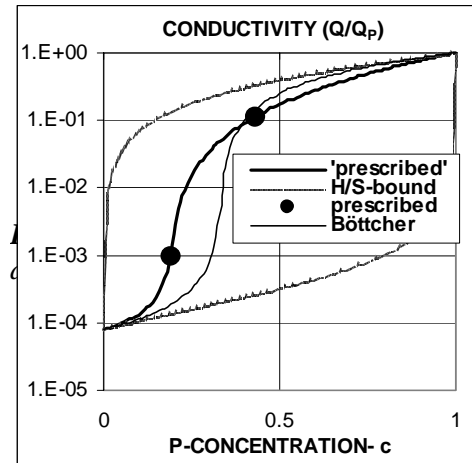


Figure 16. Conductivity analysis.

Evaluation of geometry:

The shape functions presented in Figure 15 are easily transformed to the geo-path graph shown in Figure 18. The prescribed conductivity data are properties of a composite produced with geometries described placing Figure 18 on top of the master path graph in Figure 5.

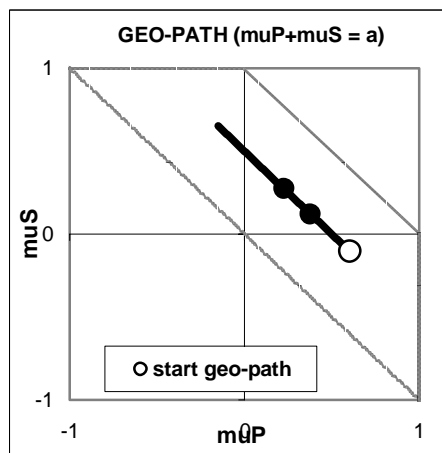


Figure 17. Geo-path in stiffness analysis

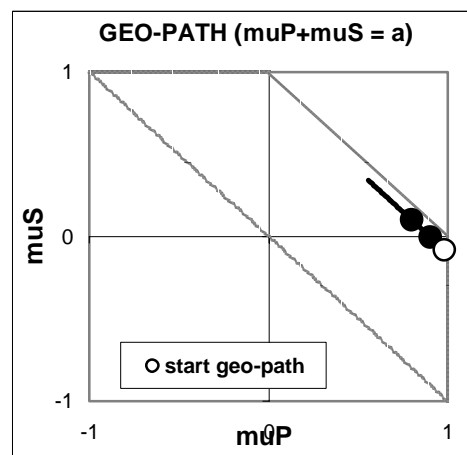


Figure 18. Geo-path in conductivity analysis

Conclusion on design aspects

A method has been presented in this paper which applies for design of composites with simple geo-paths, $\mu_S + \mu_P = a$, previously shown to apply well in property predictions for a number of composites produced with traditional technologies: Particles mixed into a continuous matrix, compaction of powders, production of porous materials, impregnation of porous materials, particulate composites with self-inflicted pores (light clinker concrete), three dimensional 'Plywood' composites.

An interesting aspect of the composite theory presented in this paper is that it offers the possibility to explore in general, how geo-paths should look to obtain prescribed material properties. This feature may act as a challenge to traditional technologies: Can we do better by new, not yet known, technologies? In order to answer this question we have to open new research projects such as the following:

- FEM tests on a number of standard composites are made - from which shape function values can be deduced at various concentrations - in principles as made in (3) for various particulate composites and so-called grid composites.
- Parallel technology studies are made on, how to produce such standard composites in practice.

Notations

Abbreviations and subscripts

V	Volume
P	Phase P
S	Phase S
no subscript	Composite materials
H/S	Hashin/Shtrikman's property bounds

Geo-parameters

$c = V_P/(V_P+V_S)$	Volume concentration of phase P
μ^o	Shape factor
μ	Shape function
c_P, c_S	Critical concentrations
θ	Geo-function for stiffness
θ_Q	Geo-function for conductivity

Stiffness and other properties

E	Stiffness (Young's modulus)
$e = E/E_S$	Relative stiffness of composite
$n = E_P/E_S$	Stiffness ratio
Q	Conductivity (e.g. thermal, electrical, chloride)
$q = Q/Q_S$	Relative conductivity of composite
$n_Q = Q_P/Q_S$	Conductivity ratio
λ	Linear eigenstrain (e.g. shrinkage, thermal expansion)
$\Delta\lambda = \lambda_P - \lambda_S$	Linear differential eigenstrain

Stress

σ	External mechanical stress
σ_P	Phase P stress caused by external mechanical stress
σ_S	Phase S stress caused by external mechanical stress
ρ	Hydrostatic stress caused by eigenstrain

Literature

1. Nielsen, L. Fuglsang: "Elastic Properties of Two-Phase Materials", *Materials Science and Engineering*, 52(1982), 39-62.
2. *Idem*: "Stiffness and other physical properties of composites as related to phase geometry and connectivity - Part I: Methods of analysis" and "- Part II: Quantification of Geometry", *3rd Symposium on Building physics in the Nordic countries, Copenhagen, sept. 13-15, 1993, pages 725-734 and 735-743 in Proceedings Vol 2 (Ed. B. Saxhof), 1993*,
3. *Idem*: "Composite Materials - Mechanical and physical behaviour as influenced by phase geometry", *Monograph R-051(2003), Department of Civil Engineering, Tech. Univ. Denmark*.
4. Hashin, Z.: "Elastic moduli of heterogeneous materials". *J. Appl. Mech.*, 29 (1962), 143 - 150.
5. Nielsen, L. Fuglsang: "Composite materials with arbitrary geometry", *Text note for Summer school on 'Hydration and Microstructure of High Performance Concrete' at the Dept. Struct. Eng. and Materials, Techn. Univ. Denmark, Lyngby, August 16-25, 1999*.
6. Hashin, Z. and Shtrikman, S.: "Variational approach to the theory of elastic behaviour of multi-phase materials". *J. Mech. Solids*, 11(1963), 127 - 140.
7. *Idem*: "A variational approach to the theory of the effective magnetic permeability of multi-phase materials", *J. Appl. Phys.* 33(1962), 3125.
8. Nielsen, L. Fuglsang: "Numerical analysis of composite materials", *Materialnyt*, 1(2001), *DSM (Danish Society for Materials Testing and Research)*.
9. Larsen, E.S. and Nielsen, C.B.: "Decay of bricks due to salt", *Materials and Structures*, 23(1990), 16 – 25.
10. Beaudoin, J.J. and R.F. Feldman: "A study of mechanical properties of autoclaved Calcium silicate systems", *Cem. Concr. Res.*, 5(1975), 103-118.
11. Feldman, R.F. and J.J. Beaudoin: "Studies of composites made by impregnation of porous bodies. I: Sulphur impregnant in Portland cement systems", *Cem. Concr. Res.*, 7(1977), 19-30.
12. Bentz, D.P., Jensen, O.M., Coats, A.M., and Glasser, F.P.: "Influence of Silica Fume on diffusivity in cement-based Materials. Part I: Experimental and computer modelling studies on cement pastes", *Submitted to Cement and Concrete Research 1999*.
13. Mejlhede Jensen, O.: Chloride ingress in cement paste and mortar measured by Electron Probe Micro Analysis", *Report R51(1999), Dept. Struct. Eng. and Materials, Tech. Univ. Denmark*
14. Nielsen, L. Fuglsang: "Strength developments in hardened cement paste – Examination of some empirical equations", *Materials and Structures*, 26(1993), 255-260.
15. Bentz, D.P., Jensen, O.M., Coats, A.M., and Glasser, F.P.: "Influence of Silica Fume on diffusivity in cement-based Materials. Part I: Experimental and computer modelling studies on cement pastes", *Submitted to Cement and Concrete Research 1999*.
16. Budiansky, B.: "On the elastic moduli of some heterogeneous materials", *J. Mech. Phys. Solids*, 13(1965), 223 - 227.